Applied Mathematics and Nonlinear Sciences 2(2) (2017) 449–464

Applied Mathematics and Nonlinear Sciences

http://journals.up4sciences.org

Bifurcation Analysis of Hysteretic Systems with Saddle Dynamics

Marina Esteban, Enrique Ponce, Francisco Torres †

Departamento de Matemática Aplicada II, Universidad de Sevilla. Escuela Técnica Superior de Ingeniería, Camino de los Descubrimientos s/n 41092
SPAIN

Submission Info

Communicated by J. Llibre
Received 6th April 2017
Accepted 4th November 2017
Available online 4th November 2017

Abstract

This paper is devoted to the analysis of bidimensional piecewise linear systems with hysteresis coming from a reduction of symmetric 3D systems with slow-fast dynamics. We concentrate our attention on the saddle dynamics cases, determining the existence of periodic orbits as well as their stability, and possible bifurcations. Dealing with reachable saddles not in the central hysteresis band, we show the existence of subcritical/supercritical heteroclinic bifurcations as well as saddle-node bifurcations of periodic orbits.

Keywords: Bifurcations, Hysteresis, Periodic Orbits.
AMS 2010 codes: 34C23, 34C55, 34C05.

1 Introduction

Following [8], hysteresis is a nonlinear phenomenon which appears in many natural and constructed systems. A system is characterized as a hysteretic system when the equations have a looping behaviour produced by a relation between two scalar time-dependent quantities that cannot be expressed in terms of a scalar function. These loops can be due to different causes, for example, the existence of thermostats for controlling the temperature, voltage threshold on a circuit, etc. In our approach, hysteretic systems appear as a consequence of dimensional reduction in the analysis of slow-fast systems, see the Appendix.

In [10] two characteristics of hysteresis are emphasized. First, the non-linearity has a dependence on previous values of the input (*memory effect*). Second, hysteretic systems undergo arbitrary quickly transitions, what is an idealization for real systems.

†Email address: marinaep@us.es, eponcem@us.es, ftorres@us.es

The mathematical analysis of hysteretic systems has emphasized its ability for generating chaotic solutions when the involved dynamics are of focus type. See [6, 7, 9]. Here, we consider instead symmetric hysteretic systems having two real equilibria of saddle type. After some preparation work, we get a canonical form which is general enough for our purpose. See the appendix for a derivation of the proposed canonical form.

We deal with an upper system of saddle type

$$\begin{cases} \dot{x} = 2\gamma(x-x_E)-(y-y_E), \\ \dot{y} = (\gamma^2-1)(x-x_E), \end{cases} \qquad x \leqslant 1, \tag{S_U}$$

and a similar lower system, namely

$$\begin{cases} \dot{x} = 2\gamma(x+x_E)-(y+y_E), \\ \dot{y} = (\gamma^2-1)(x+x_E), \end{cases} \qquad x \geqslant -1, \tag{S_L}$$

plus some hysteretic transition mechanism, to be specified later, that allows to build continuous solutions for the global system. Note that, due to the features of our system, we cannot take advantage of any local method for the analysis of dynamics, as done in [5] looking for the characterization of centers in planar dynamical systems. Here, as usual, the dot represents derivatives with respect to the time τ, (x_E, y_E) and $(-x_E, -y_E)$ are the equilibria for the S_U-system and S_L-system respectively. In order to get a dynamics of saddle type we must choose $\gamma \in (-1,1)$.

Next we define the solutions of the global system (S_U)-(S_L) by using the following transition mechanism. Take $(x(0), y(0))$ with $x(0) < 1$ as the initial condition of a solution $(x(\tau), y(\tau))$ of the S_U-system. Then this solution is called a *valid solution* as long as $x(\tau) \leqslant 1$. If there exists a time τ_f, such that $x(\tau_f) = 1$ with $\dot{x} > 0$, then the point $(x(\tau_f), y(\tau_f))$ is assumed to be the initial point for an orbit of the S_L-system and this orbit continues by integrating system (S_L) .

Analogously, any solution $(x(\tau), y(\tau))$ of the S_L-system with $x(0) > -1$, is considered as a *valid solution* as long as $x(\tau) > -1$, and if there exists a time τ_r such that $x(\tau_r) = -1$ with $\dot{x}(\tau_r) < 0$, then the point $(x(\tau_r), y(\tau_r))$ is assumed to be the initial point for an orbit of the S_U-system.

In passing from the S_U-system to the S_L-system, we speak of a *fall*, which occurs when an orbit of the system (S_U), called upper orbit, hits the falling line

$$\Sigma_+ = \{(x,y) : x = 1\}.$$

Similarly, we define a *rise* when we pass from the S_L-system to the S_U-system, which occurs when an orbit of system (S_L), called lower orbit, intersects the rising line

$$\Sigma_- = \{(x,y) : x = -1\}.$$

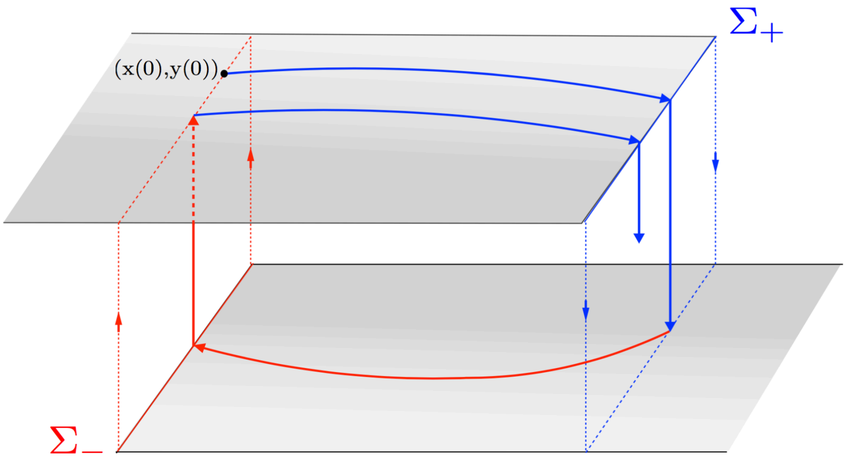

Fig. 1 The transition mechanism between systems (S_U) and (S_L). We use blue colour for solutions of the upper system and red colour for solutions of the lower one. We can see also the falls at the line Σ_+ and the rises at the line Σ_-.

Note that our formulation is equivalent to write the system

$$\begin{cases} \dot{x} = 2\gamma x - y - H(x)(2\gamma x_E - y_E), \\ \dot{y} = (\gamma^2 - 1)(x - H(x)x_E), \end{cases}$$

where $H(x)$ is the standard normalized hysteretic function of Figure 2.

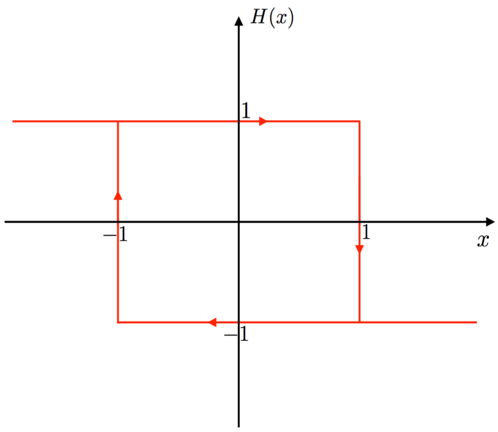

Fig. 2 The 'graph' of a normalized hysteresis function. The hysteresis value $H(x)$ is unambiguous for $x < -1$ and $x > 1$. However, for $-1 \leqslant x \leqslant 1$ the output depends on the past, as explained in the text.

Thus, any periodic orbit of global system (S_U)-(S_L) will lead to a repeated sequence of falls and rises and has at least two pieces, one corresponding to an orbit of system (S_U) and the other to an orbit of system (S_L).

There is no loss of generality in taking the initial point of a periodic orbit to belong to an orbit of the upper system. In particular, in what follows we assume $x(0) = -1$, so that our initial point will be $(-1, u_-) \in \Sigma_-$, on the rising line, for a certain $u_- \in \mathbb{R}$. Our strategy is to look for the first point where the orbit of the upper system arrives at Σ_+, the falling line, in a point $(1, u_+)$. Thus, we can define an evolution map

$$\begin{aligned} T_U : \Sigma_-^{ad} \subset \Sigma_- \;&\rightarrow\; \Sigma_+ \\ (-1, u_-) &\longmapsto (1, u_+) \end{aligned}$$

where Σ_-^{ad} represents the admissible subset of points in Σ_- for which the forward orbits of the S_U-system reach Σ_+ and fall. This function induces a scalar map U, such that $u_+ = U(u_-)$, which will be called the transition map.

A similar evolution map can be defined for the S_L-system by considering the points $(1, l_+) \in \Sigma_+^{ad} \subset \Sigma_+$ whose forward orbits reach Σ_- and rise, namely

$$\begin{aligned} T_L : \Sigma_+^{ad} \subset \Sigma_+ &\to \Sigma_- \\ (1, l_+) &\longmapsto (-1, l_-) \end{aligned}$$

This map also induces a transition map L, which is defined by $l_- = L(l_+)$.

Clearly, the full transition map for the global system (S_U)-(S_L) will be the composition of both maps U and L, that is $L \circ U$, provided that such composition is possible. Obviously, if for a given u_- we have that $u_+ = U(u_-)$ belongs to the domain of L, we can take $l_+ = u_+$ and compute the value $L(l_+) = l_-$. Then, the condition $l_- = u_-$ is equivalent to the existence of a periodic orbit.

Once introduced the systems under study and having defined in a precise way how the different orbits behave, our goal is to analyze the existence of periodic orbits and characterize their bifurcations. To this end, after some preliminary results that appear in Section 2, we present our main results in Section 3, see Theorem 9. Such theorem implies that, in the particular saddle case under study, periodic orbits appear either through heteroclinic bifurcations or through saddle-node bifurcations. Furthermore, we show that all the periodic orbits are symmetric, that its maximum number is two, and that at least one of them is stable.

For sake of brevity, the included study of hysteretic symmetric systems with saddle dynamics only considers the case of real saddles out of the hysteresis band, that is $x_E < -1$. The remaining cases, namely real saddles in the central band ($|x_E| \leqslant 1$) and virtual saddles ($x_E > 1$) will appear elsewhere.

2 Preliminary results

The symmetry between the S_U-system and the S_L-system imposes a symmetry property for the functions L and U as follows.

Proposition 1. *The following statements hold.*

(a) If $U(y)$ is well-defined, then $L(-y)$ is well-defined and $L(-y) = -U(y)$.

(b) The full transition map satisfies $L \circ U = (-U) \circ (-U)$.

Proof. We only show the first assertion. Under the hypothesis, taking $v = U(y)$, we know that

$$T_U(-1, y) = (1, v).$$

Since the S_L-system is the symmetric one of the S_U-system with respect to the origin, we have

$$T_L(1, -y) = (-1, -v),$$

and so $-v = L(-y)$ and we are done.

Assume that we start from a point $(-1, u_-) \in \Sigma_-^{ad}$ so that $T_U(-1, u_-) = (1, u_+)$. Clearly, if $(1, u_+) \in \Sigma_+^{ad}$ and $T_L(1, u_+) = (-1, u_-)$ we have a periodic orbit. In other words, we must have

$$\begin{cases} U(u_-) = u_+, \\ L(u_+) = u_-. \end{cases} \tag{1}$$

Reciprocally, if equations (1) have a solution pair (u_-, u_+), then there exists an associated periodic orbit.

Although periodic orbits of four (or more) transitions could be possible, in principle, we omit its consideration in the sequel, and so, when we speak of periodic orbits, we will assume that they have only two transitions.

If we assume that (u_-, u_+) is a solution pair of (1), the following result is straightforward.

Proposition 2. *Periodic orbits of global system (S_U)-(S_L) come in pairs, excepting the case where the periodic orbit is symmetrical with respect to the origin.*

Proof. Starting from a solution pair (u_-, u_+) of (1), and applying Proposition 1, we can write,

$$L(-u_-) = -U(u_-) = -u_+,$$
$$U(-u_+) = -L(u_+) = -u_-,$$

and reordering equations, we conclude that the pair $(-u_+, -u_-)$ is also a solution of (1), so that there exists a companion periodic orbit, which is the symmetric one of the assumed periodic orbit with respect to the origin. In the particular case where $u_+ = -u_-$, the periodic orbit is itself symmetrical with respect to the origin, and the proof is complete.

Corollary 3. *The existence of a pair of non-symmetric periodic orbits implies, by a standard application of the intermediate value theorem to the function $U(y)+y$, the existence of a third symmetric periodic orbit.*

For the specific case of symmetric periodic orbits, instead of equations (1), we must only consider the equation

$$U(u) = -u, \tag{2}$$

so that any solution of (2) represents a symmetric periodic orbit.

Regarding the stability, a periodic orbit is stable if the absolute value of the derivative of the full transition map is less than one at the fixed point. Taking into account Proposition 1 (b), we get $(L\circ U)'(u) = U'(u)^2$ whenever (2) is fulfilled, and so we deduce stability for a symmetric periodic orbit if

$$|U'(u_-)| < 1, \tag{3}$$

being u_- the fixed point.

In any case, according to Proposition 1, we only need to study the transition map U. To this end, let us write the explicit solutions of system (S_U) taking into account that the equilibria is of saddle type, namely

$$\begin{pmatrix} x(\tau)-x_E \\ y(\tau)-y_E \end{pmatrix} = e^{\gamma\tau} \begin{pmatrix} \mathrm{ch}\tau+\gamma\mathrm{sh}\tau & -\mathrm{sh}\tau \\ (\gamma^2-1)\mathrm{sh}\tau & \mathrm{ch}\tau-\gamma\mathrm{sh}\tau \end{pmatrix} \begin{pmatrix} x(0)-x_E \\ y(0)-y_E \end{pmatrix}. \tag{4}$$

Note that we use the abridged notation $\mathrm{ch}\tau$, $\mathrm{sh}\tau$ for $\mathrm{ch}(\tau)$ and $\mathrm{sh}(\tau)$ respectively, for convenience.

For the system (S_U), the stable and unstable manifold of the saddle equilibrium (x_E, y_E) are

$$y = y_E + (\gamma+1)(x-x_E), \quad y = y_E + (\gamma-1)(x-x_E)$$

respectively.

In this work, we assume in the sequel $x_E < -1$, corresponding to the case when the saddle of system (S_U) is on the left of Σ_-. Now, we define the domain of the transition map T_U, Σ_-^{ad}, by introducing some distinguished points.

Definition 1. For $x_E < -1$ let us introduce the points $(-1, u_-^*)$, where the stable manifold of the saddle intersects Σ_-, and the contact point $(-1, \hat{u}_-)$ of system (S_U) with Σ_-, that is the point of Σ_- where $\dot{x} = 0$. Simple computations lead to

$$u_-^* = y_E - (\gamma+1)(x_E+1), \quad \hat{u}_- = y_E - 2\gamma(x_E+1).$$

We also introduce the point $(-1,u_-^*)$ where the stable manifold of the saddle intersects Σ_-, and the point $(-1,\hat{u}_+)$ where the orbit tangent to Σ_- at $(-1,\hat{u}_-)$ reaches Σ_+. We get

$$u_+^* = y_E - (\gamma-1)(x_E-1), \quad \hat{u}_+ = U(\hat{u}_-).$$

See Figure 3 for a geometrical view of these distinguished points.

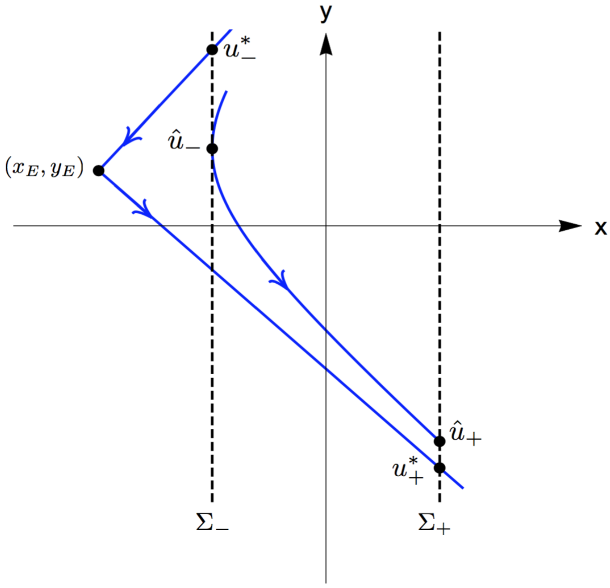

Fig. 3 The saddle point (x_E, y_E) and its invariant manifolds for the upper system (S_U). Other distinguished values are emphasized.

Accordingly, we get as the admissible domain for the map T_U the set

$$\Sigma_-^{ad} = \{(-1,u_-) : u_- < u_-^*\},$$

so the map U is defined in the interval $u_- < u_-^*$. In fact, as we will see later, the map U is not injective in such interval, unless we restrict the domain to the subset with $u_- \leqslant \hat{u}_-$.

Since it is not possible to write an explicit expression of u_+ in terms of u_-, we obtain the parametric expression of the transition map U in terms of the flight time τ, by considering a starting point $(-1,u_-) \in \Sigma_-^{ad}$ and imposing that the orbit corresponding to this point reaches Σ_+ in a point $(1,u_+)$. We follow so a similar approach to the one introduced in [2] for a different case. So, using the expression (4), we get

$$\begin{aligned} u_-(\tau) &= y_E + \frac{e^{-\gamma\tau}(x_E-1) - (x_E+1)(\mathrm{ch}\tau + \gamma\mathrm{sh}\tau)}{\mathrm{sh}\tau}, \\ u_+(\tau) &= y_E - \frac{e^{\gamma\tau}(x_E+1) - (x_E-1)(\mathrm{ch}\tau - \gamma\mathrm{sh}\tau)}{\mathrm{sh}\tau}. \end{aligned} \tag{5}$$

Now, we write the first and second derivatives with respect to τ, to be used later,

$$\begin{aligned} u_-'(\tau) &= \frac{(x_E+1) - (x_E-1)e^{-\gamma\tau}(\mathrm{ch}\tau + \gamma\mathrm{sh}\tau)}{\mathrm{sh}^2\tau}, \\ u_+'(\tau) &= \frac{-(x_E-1) + (x_E+1)e^{\gamma\tau}(\mathrm{ch}\tau - \gamma\mathrm{sh}\tau)}{\mathrm{sh}^2\tau}, \end{aligned} \tag{6}$$

and

$$u''_-(\tau) = \frac{-2(x_E+1)\text{ch}\tau + (x_E-1)e^{-\gamma\tau}(1+(\text{ch}\tau+\gamma\text{sh}\tau)^2)}{\text{sh}^3\tau},$$
$$u''_+(\tau) = \frac{2(x_E-1)\text{ch}\tau - (x_E+1)e^{-\gamma\tau}(1+(\text{ch}\tau-\gamma\text{sh}\tau)^2)}{\text{sh}^3\tau}. \tag{7}$$

Standard computations show that

$$\lim_{\tau\to 0} u_-(\tau) = \lim_{\tau\to 0} u_+(\tau) = -\infty,$$

and

$$\lim_{\tau\to\infty} u_-(\tau) = u_-^*, \quad \lim_{\tau\to\infty} u_+(\tau) = u_+^*.$$

Using the parametric expressions (5), the condition for the existence of symmetric periodic orbits (2), in terms of u_- and u_+ is

$$u_-(\tau) + u_+(\tau) = 0.$$

On the other hand, for a non-symmetric periodic orbit of the global system, we have two different flight times τ_1 and τ_2, corresponding to the (S_U) and (S_L) pieces of the orbit, respectively. So, a non-symmetric periodic orbit has to verify in terms of u_- and u_+ the following equations

$$\begin{cases} u_-(\tau_2) + u_+(\tau_1) = 0, \\ u_-(\tau_1) + u_+(\tau_2) = 0. \end{cases} \tag{8}$$

The condition (3) for the stability of a symmetric periodic orbit, in terms of u_- and u_+, results in

$$|U'(u_-)| = \left|\frac{u'_+(\tau)}{u'_-(\tau)}\right| < 1.$$

In the case of non-symmetric periodic orbit, to compute the derivative of the full transition map $L \circ U$, we start by using the notation $p = u_-(\tau_1)$, $q = u_+(\tau_1) = -u_-(\tau_2)$ to write

$$\begin{aligned} \tfrac{d}{dp}(L\circ U)(p) &= L'(U(p))U'(p) = L'(q)U'(p) = \\ &= U'(-q)U'(p) = U'(u_-(\tau_2))U'(u_-(\tau_1)), \end{aligned}$$

where we have used that $L(q) = -U(-q)$. Now, the stability of a periodic orbit requires

$$|U'(u_-(\tau_2))U'(u_-(\tau_1))| = \left|\frac{u'_+(\tau_1)u'_+(\tau_2)}{u'_-(\tau_1)u'_-(\tau_2)}\right| < 1.$$

It will be useful to introduce the auxiliary parameter

$$\rho = \frac{x_E+1}{x_E-1},$$

which belongs to the interval $(0,1)$ since $x_E < -1$.

The following lemmas give preliminary properties to be used later.

Lemma 4. *For $x_E < -1$ and $\gamma \in (-1,1)$, the function $u_-(\tau)$ is increasing for all $\tau \in (0,+\infty)$.*

Proof. From (6), we see that

$$\operatorname{sign}(u'_-(\tau)) = \operatorname{sign}(e^{-\gamma\tau}(\operatorname{ch}\tau + \gamma\operatorname{sh}\tau) - \rho),$$

and then, to get the conclusion, as $\rho \in (0,1)$, it suffices to see that

$$\eta(\tau) = e^{-\gamma\tau}(\operatorname{ch}\tau + \gamma\operatorname{sh}\tau) \geqslant 1, \quad \text{for all } \tau \geqslant 0.$$

Effectively, since $\eta(0) = 1$, and $\eta'(\tau) = (1-\gamma^2)e^{-\gamma\tau}\operatorname{sh}\tau > 0$, we are done.

Lemma 5. *For $x_E < -1$ and $\gamma \in (-1,1)$, the transition map U defined in (5) is concave down.*

Proof. The transition map U is concave down if and only if

$$U''(u_-) = \frac{u'_-u''_+ - u''_-u'_+}{(u'_-)^3} < 0, \text{ for all } \tau \in (0,+\infty),$$

where we omit the argument in the above functions for brevity.

From Lemma 4, $u'_- > 0$ and so, we need to study the sign of

$$u'_-u''_+ - u''_-u'_+ = \frac{(1-\gamma^2)(e^{2\gamma\tau}\rho^2 - 2\gamma\rho e^{\gamma\tau}\operatorname{sh}\tau - 1)}{\operatorname{sh}^3\tau}.$$

The conclusion comes from the fact that $e^{2\gamma\tau}\rho^2 - 2\gamma\rho e^{\gamma\tau}\operatorname{sh}\tau - 1$ is a quadratic polynomial in ρ negative for $\rho \in (0,1)$, and we are done.

3 Main results for real saddles out of the hysteresis band

Our objective is to study the existence, uniqueness and stability of the possible periodic orbits. Our first result gives two necessary conditions for the existence of non-symmetric periodic orbits.

Lemma 6. *(Necessary conditions for non-symmetric periodic orbits)*
If there exists a non-symmetric periodic orbit, the two following statements are true.

(a) The function $u_+(\tau) - u_-(\tau)$ is not injective.

(b) The function $u_+(\tau) + u_-(\tau)$ takes opposite values.

Proof. Adding and subtracting equations (8), we can write

$$\begin{aligned} u_+(\tau_1) - u_-(\tau_1) &= u_+(\tau_2) - u_-(\tau_2), \\ u_+(\tau_1) + u_-(\tau_1) &= -[u_+(\tau_2) + u_-(\tau_2)], \end{aligned}$$

and the conclusion follows.

Proposition 7. *When $x_E < -1$ and $\gamma \in (-1,1)$, there cannot be non-symmetric periodic orbits.*

Proof. Let us show that the function $u_+(\tau) - u_-(\tau)$ is injective and so the conclusion will follow from Lemma 6. We will show that $u'_+(\tau) - u'_-(\tau) < 0$ for all $\tau > 0$.

From (6), we see that

$$\operatorname{sign}[u'_+(\tau) - u'_-(\tau)] = \operatorname{sign}[(x_E+1)\xi(\tau;\gamma) + (x_E-1)\xi(\tau;-\gamma)],$$

where $\xi(\tau;\gamma) = e^{\gamma\tau}(\operatorname{ch}\tau - \gamma\operatorname{sh}\tau) - 1$. Since $\xi(0;\gamma) = 0$ and $\xi'(\tau;\gamma) = e^{\gamma\tau}(1-\gamma^2)\operatorname{sh}\tau > 0$, we conclude that $u'_+(\tau) - u'_-(\tau) < 0$ for all $\tau > 0$, and the conclusion follows.

Proposition 8. *Consider system (S_U)-(S_L) with $x_E < -1$ and $\gamma \in (-1,1)$ fixed. The maximum number of periodic orbits is two and all of them are symmetric.*

Proof. From Proposition 7, there can be only symmetric periodic orbits. By equation (2), the number of symmetric periodic orbits of the global system correspond to the intersections of the transition map U with the secondary diagonal. Since the map U is concave down from Lemma 5, we conclude that the maximum number of symmetric periodic orbits is two.

In what follows, we assume a fixed value x_E for the abscissa of the saddle point, and we study equation (2) looking for the solution values of y_E, γ and τ. It is worth noting that the effect of the parameter y_E in (5) is only a translation.

Next, by considering γ and y_E as principal bifurcation parameters, we give the complete bifurcation set for the case $x_E < -1$. We classify the parameter regions according to the number of symmetric periodic orbits, see Figure 4. The case $x_E \geqslant -1$ will be the subject of future works.

Theorem 9. *Consider system (S_U)-(S_L) with $x_E < -1$ and $\gamma \in (-1,1)$ fixed. The following statements hold.*

(a) If we define the function $y_H(\gamma) = 1 + \gamma x_E$, then at the points of the straight line $y_E = y_H(\gamma)$ in the parameter plane (γ, y_E), the system has an heteroclinic bifurcation.

For $\gamma \in (-1,0]$ this bifurcation is supercritical, namely, for $y_E > y_H(\gamma)$ the heteroclinic connection gives rise to a stable symmetric periodic orbit.

For $\gamma \in (0,1)$ the bifurcation is subcritical, so that when $y_E = y_H(\gamma)$ the heteroclinic connection coexists with a stable symmetric periodic orbit, while for $y_E < y_H(\gamma)$ the heteroclinic connection gives rise to an unstable symmetric periodic orbit that coexists with the stable one.

Furthermore, for $y_E > y_H(\gamma)$ there exists only one stable symmetric periodic orbit.

(b) For $\gamma \in (-1,0]$ and $y_E < y_H(\gamma)$ there are no periodic orbits. For $\gamma \in (0,1)$, there exists a function $y_{SN}(\gamma)$ such that $y_{SN}(\gamma) < y_H(\gamma)$ and

$$\lim_{\gamma \to 0^+} y_{SN}(\gamma) = 1, \quad \lim_{\gamma \to 1^-} y_{SN}(\gamma) = 2(x_E + 1),$$

so that at the points $(\gamma, y_{SN}(\gamma))$, the system undergoes a saddle-node bifurcation of symmetric periodic orbits. More precisely, when $\gamma \in (0,1)$ in the interval

$$y_{SN}(\gamma) < y_E < y_H(\gamma)$$

the system has two symmetric periodic orbits with opposite stability, while for $y_E < y_{SN}(\gamma)$ there are no periodic orbits.

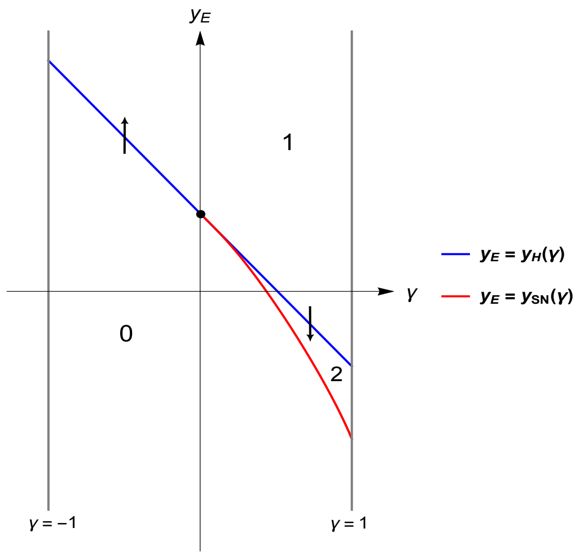

Fig. 4 Bifurcation set in the parameter plane (γ, y_E) for $x_E < -1$. We emphasized the number of symmetric periodic orbits in each region.

Proof. Since symmetric periodic orbits correspond with the intersections of the graph of U with the secondary diagonal of the plane (u_-, u_+), some properties of map U are studied. To prove the theorem, we distinguish the two cases $\gamma \in (-1,0]$ and $\gamma \in (0,1)$.

When $\gamma \in (-1,0]$, from Lemmas 4 and 5 the map U satisfies

$$\lim_{u_- \to u_-^*} U(u_-) = u_+^*, \quad U''(u_-) < 0, \text{ for all } u_- < u_-^*.$$

In the open interval $\gamma \in (-1,0)$, we have also

$$0 < U'(u_-) < 1, \quad \lim_{u_- \to u_-^*} U'(u_-) = 0;$$

while, in the particular case $\gamma = 0$,

$$-\rho < U'(u_-) < 1, \quad \lim_{u_- \to u_-^*} U'(u_-) = -\rho.$$

In Figure 5, the above properties are illustrated.

The heteroclinic connection arises when $u_+^* = -u_-^*$, and taking into account Definition 1, we get the expression $y_H(\gamma) = 1 + \gamma x_E$. Since $U'(u_-) > -1$ for $\gamma \in (-1,0]$, it is not possible to get a tangent point of the map U with the line $u_+ = -u_-$. Then, the maximum number of symmetric periodic orbits is one in this case. So, for $\gamma \in (-1,0]$ we have the following situations.

(a) If $y_E < y_H(\gamma)$, then there are no periodic orbits because the map U does not intersect with $u_+ = -u_-$.

(b) If $y_E = y_H(\gamma)$, then the heteroclinic connection is produced.

(c) If $y_E > y_H(\gamma)$, then there is a stable symmetric periodic orbit because the map U has exactly an intersection point with the secondary diagonal.

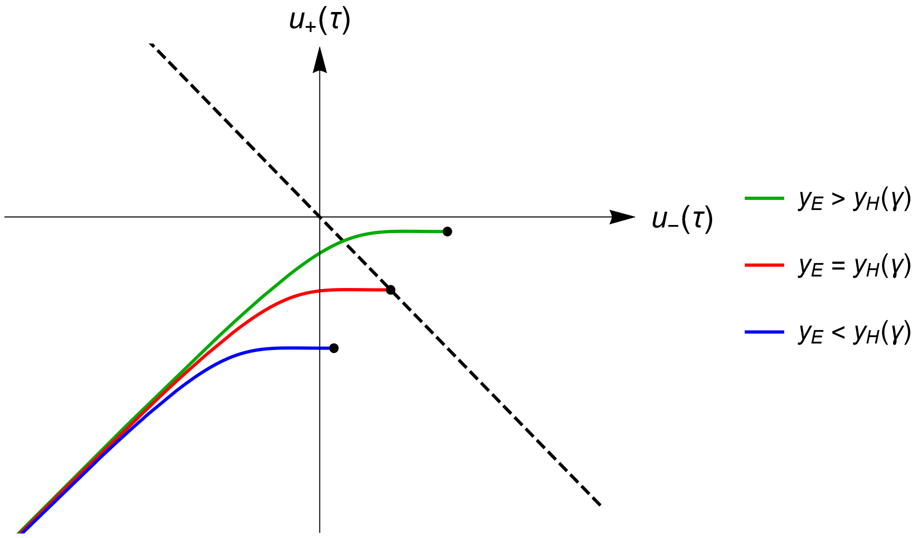

Fig. 5 The transition map U for different values of the parameter y_E and $\gamma \in (-1,0)$. The black points in this figure represent the point $u^* = (u_-^*, u_+^*)$ for each case.

When $\gamma \in (0,1)$ the situation is more involved, due to the lack of injectivity for the map U and the fact that its derivative $U'(u_-)$ can be -1, see Figure 6. We still have $U''(u_-) < 0$ for all $u_- < u_-^*$ but we now have $U'(\hat{u}_-) = 0$, so that

$$0 < U'(u_-) < 1, \text{ for all } u_- < \hat{u}_-, \text{ and } U'(u_-) < 0, \text{ for all } u_- > \hat{u}_-,$$

along with

$$\lim_{u_- \to u_-^*} U(u_-) = u_+^*, \quad \lim_{u_- \to u_-^*} U'(u_-) = -\infty.$$

From now on, we emphasize the dependence of γ for the functions. The heteroclinic connection is obtained as before, while the saddle-node bifurcation comes from applying the saddle-node theorem in [4]. This theorem assures the existence of a saddle-node bifurcation of periodic orbits under several conditions for the map $G := U(-U(u_-;\gamma);\gamma) + u_-$, which can be translated to the map U as follows.

(a) Periodic orbit condition: $U(u_-;\gamma) = -u_-$,

(b) Non-hyperbolicity condition: $U'(u_-;\gamma) = -1$,

(c) Transversality condition: $\dfrac{\partial U}{\partial \gamma}(u_-;\gamma) \neq 0$,

(d) Non-degeneracy condition: $U''(u_-;\gamma) \neq 0$.

Since we have the expression of the transition map U in a parametric form, the above conditions are equivalent to

(a) $u_+(\tau;\gamma) + u_-(\tau;\gamma) = 0$,

(b) $u'_+(\tau;\gamma) + u'_-(\tau;\gamma) = 0$,

(c) $\dfrac{\partial u_+}{\partial \gamma}(\tau;\gamma) + \dfrac{\partial u_-}{\partial \gamma}(\tau;\gamma) \neq 0$ and

(d) $u''_+(\tau;\gamma) + u''_-(\tau;\gamma) \neq 0$.

Next, we study the equations (a) and (b) in order to check if their solutions satisfy the other two conditions (c) and (d). In such a case, the global system (S_U)-(S_L) undergoes a saddle-node bifurcation of periodic orbits for the obtained values of the parameters.

After some computations, we get that condition (a) is equivalent to

$$(y_E - \gamma x_E)\mathrm{sh}\tau = \mathrm{ch}\tau + \mathrm{ch}(\gamma\tau) + x_E \mathrm{sh}(\gamma\tau), \tag{9}$$

and condition (b) can be rewritten as $f(\tau) = \rho$, where

$$f(\tau) := \frac{e^{-\gamma\tau}(\mathrm{ch}\tau + \gamma\mathrm{sh}\tau) + 1}{e^{\gamma\tau}(\mathrm{ch}\tau - \gamma\mathrm{sh}\tau) + 1} = \frac{x_E + 1}{x_E - 1} = \rho. \tag{10}$$

Now, we study if the equation (10) has a solution for each $\gamma \in (0,1)$.

Some properties of $f(\tau)$ are

$$f(0) = 1, \quad \lim_{\tau \to +\infty} f(\tau) = 0.$$

Also, standard computations show that for $\gamma \in (0,1)$, the function f is positive and decreasing. Then, there is only one solution of (10), in other words, there is only one point of the map U which has slope -1. Finally, we also need to check the conditions (c) and (d) for the solution obtained before. Condition (c) is equivalent to

$$-\frac{2x_E\mathrm{sh}\tau + \gamma(e^{\gamma\tau}(x_E+1) + e^{-\gamma\tau}(x_E-1))}{\mathrm{sh}\tau} \neq 0,$$

which is automatically satisfied for $\gamma \in (0,1)$ and $\tau > 0$.

Condition (d) is more involved and we prove it by contradiction. Using equations (7), to deny condition (d) is equivalent to assume the equality

$$\begin{gathered} -2(x_E+1)\mathrm{ch}\tau + e^{-\gamma\tau}(x_E-1)(1+(\mathrm{ch}\tau+\gamma\mathrm{sh}\tau)^2) + \\ 2(x_E-1)\mathrm{ch}\tau - e^{\gamma\tau}(x_E+1)(1+(\mathrm{ch}\tau-\gamma\mathrm{sh}\tau)^2) = 0. \end{gathered}$$

Dividing by $(x_E - 1)$, and using condition (b) we get

$$e^{-\gamma\tau}(1-\gamma^2)\mathrm{sh}^2\tau(-2\gamma e^{\gamma\tau}\mathrm{sh}\tau - e^{2\gamma\tau} + 1) = 0,$$

which is a contradiction because all the factors are non-vanishing.

To get the saddle-node curve $y_E = y_{SN}(\gamma)$, shown in Figure 4, we fix $\gamma \in (0,1)$ and solve equation (10) for τ. Assume that τ^* is that solution. Then, we put τ^* in (9) and we obtain only one solution $y_E = y_{SN}(\gamma)$. For this concrete value of y_E, the point of the map U with slope -1 is exactly on the line $u_+(\tau) + u_-(\tau) = 0$. As a consequence, perturbing slightly the parameter y_E, we have either no symmetric periodic orbits when $y_E < y_{SN}(\gamma)$ or two of them if $y_E > y_{SN}(\gamma)$.

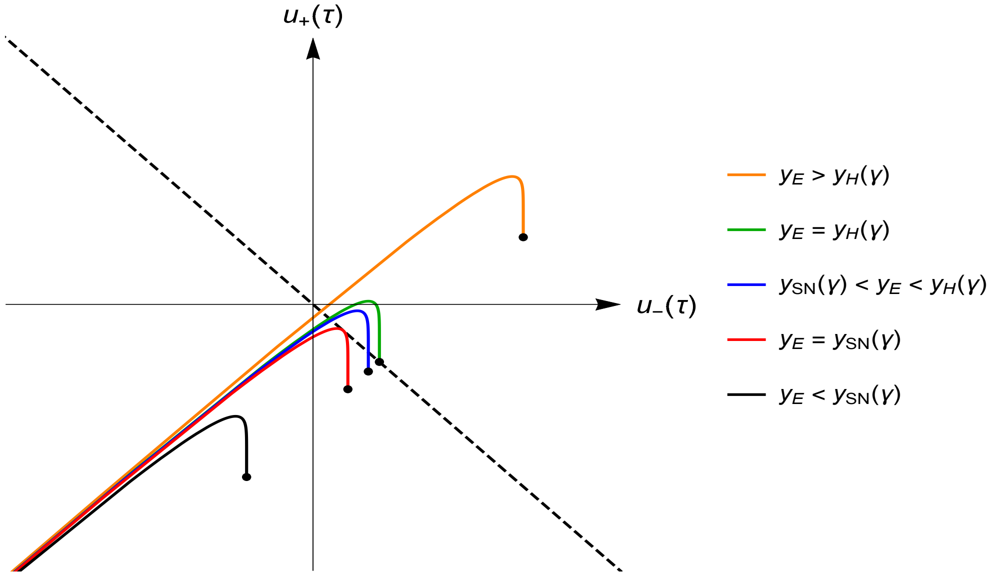

Fig. 6 The transition map U for different values of y_E. Again, the terminal black points in this figure represent the point $u^* = (u_-^*, u_+^*)$ for each case.

We show in Figure 7 two symmetric periodic orbits coexisting for $\gamma \in (0,1)$ and $y_{SN}(\gamma) < y_E < y_H(\gamma)$. This parameter region is indicated in Figure 4.

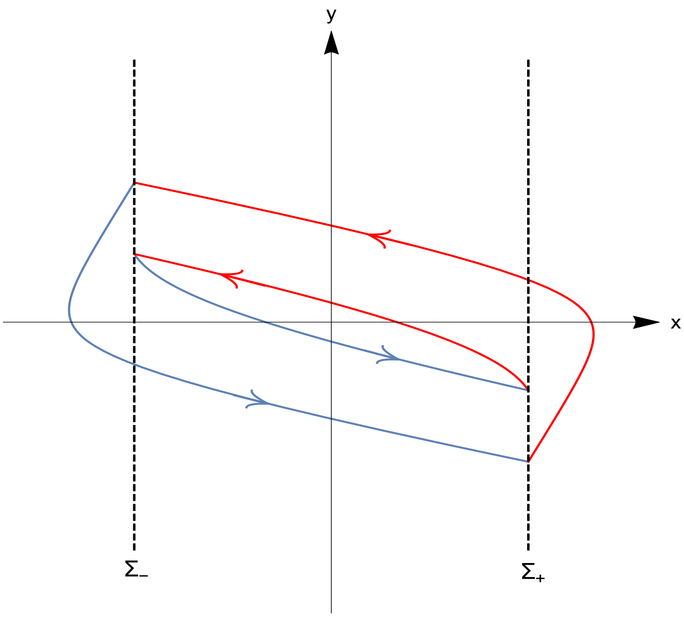

Fig. 7 The two symmetric periodic orbits existing for $(x_E, y_E) = (-2, -1)$ and $\gamma = 0.8$. One of them takes the three zones and is unstable. The other one takes only the central zone and is stable. The blue lines (resp. red lines) correspond to valid solutions for the S_U-system (resp. S_L-system).

4 Conclusions

The dynamical richness regarding the existence of periodic orbits in bidimensional hysteretic linear systems with symmetry, for the specific case of equilibria not in the hysteretic band, has been shown through a bifurcation analysis. The corresponding bifurcation set is mainly organized by a locus of heteroclinic bifurcations, what indicates the relevance of heteroclinic orbits, as it has been recently emphasized in this journal, see [1]. The bifurcation set also includes a locus of saddle-node bifurcations of periodic orbits, leading to a parameter region where two different periodic orbits coexist.

Acknowledgements

Authors are partially supported by the *Spanish Ministerio de Economía, Industria y Competitividad*, in the frame of projects MTM2014-56272-C2-1-P and MTM2015-65608-P, and by the *Consejería de Economía y Conocimiento* de la Junta de Andalucía under grant P12-FQM-1658.

5 Appendix: From 3D slow-fast systems to 2D hysteretic systems

We start by assuming a symmetric 3D piecewise linear system with the following structure

$$\begin{aligned} \begin{pmatrix} \dot{X} \\ \dot{Y} \end{pmatrix} &= A \begin{pmatrix} X \\ Y \end{pmatrix} + \mathbf{b}Z, \\ \varepsilon \dot{Z} &= -X + \varphi(Z), \end{aligned} \tag{3DPWL}$$

where $X, Y, Z \in \mathbb{R}$ are the states variables, $A = (a_{ij})$ is a 2×2 matrix with coefficients in $\mathbb{R}$, $\mathbf{b} = (b_1, b_2)^T$ is a real vector, $0 < \varepsilon \ll 1$ and $\varphi(Z)$ is a piecewise linear function defined by

$$\varphi(Z) = \begin{cases} -m(Z+z_0) - x_0, & Z \leqslant -z_0, \\ cZ, & |Z| \leqslant z_0, \\ -m(Z-z_0) + x_0, & Z \geqslant z_0, \end{cases}$$

where c, m, x_0 and z_0 are positive real numbers, and $x_0 = cz_0$ so that $\varphi(Z)$ is a continuous function. Here, the dot represents the derivative with respect to the time s.

In the limit when $\varepsilon \to 0$, the last equation of (3DPWL) represents a surface which is usually called *slow manifold*. In Figure 8 we can see a graph of $\varphi(Z)$ and the generated surface for some values of the parameters c, m, x_0 and z_0.

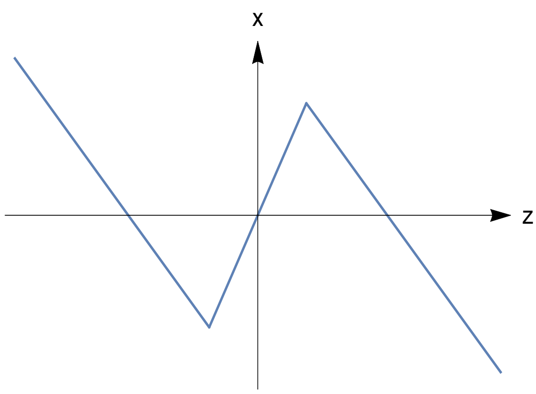

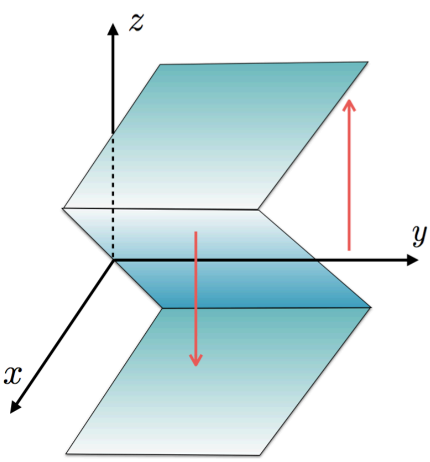

Fig. 8 *Typical graph for $\varphi(Z)$ and surface $X = \varphi(Z)$.*

Regarding Figure 8, we can define the two half-planes $\mathbf{Z_U}$ and $\mathbf{Z_L}$, namely

$$\mathbf{Z_U} = \{(X,Y,Z) \in \mathbb{R}^3 : X - x_0 + m(Z - z_0) = 0, X \leqslant x_0\},$$
$$\mathbf{Z_L} = \{(X,Y,Z) \in \mathbb{R}^3 : X + x_0 + m(Z + z_0) = 0, X \geqslant -x_0\}.$$

The set, $\mathbf{Z_U}$ (resp. $\mathbf{Z_L}$) will be called upper half-plane (resp. lower half-plane). Now, for $\delta \neq 0$ and small, consider a half-plane which is parallel to $\mathbf{Z_U}$

$$\Pi = \{(X,Y,Z) \in \mathbb{R}^3 : X - x_0 + m(Z - z_0) = \delta, X \leqslant x_0\}.$$

Then, using the last equation of (3DPWL) with the suitable evaluation of

$$\operatorname{sign}(\dot{\delta}) = -\operatorname{sign}(\delta),$$

and so, $\mathbf{Z_U}$ is attractive. Something similar occurs for the lower half-plane $\mathbf{Z_L}$. However, the intermediate stripe between $\mathbf{Z_U}$ and $\mathbf{Z_L}$ turns out to be repulsive.

Therefore, we can consider that the motion in $\mathbb{R}^3$ happens only in the two attractive half-planes $\mathbf{Z_U}$ and $\mathbf{Z_L}$ (upper and lower). When an orbit reaches the boundary of one half-plane ($\mathbf{Z_U}$ or $\mathbf{Z_L}$), it jumps instantaneously to the other half-plane by keeping the same values of X and Y and changing only the value of Z. Clearly, the dynamics on each half-plane is essentially two-dimensional; in fact, we can eliminate the third variable by projecting the orbits on the plane $Z = 0$ by using the equation of each half-plane. Then we have on $\mathbf{Z_U}$ for $Z \geqslant z_0$, the dynamical system

$$\begin{pmatrix} \dot{X} \\ \dot{Y} \end{pmatrix} = \widetilde{A} \begin{pmatrix} X \\ Y \end{pmatrix} + \widetilde{\mathbf{b}}, \qquad \text{if } X \leqslant x_0,$$

and similarly on $\mathbf{Z_L}$ for $Z \leqslant -z_0$, the system

$$\begin{pmatrix} \dot{X} \\ \dot{Y} \end{pmatrix} = \widetilde{A} \begin{pmatrix} X \\ Y \end{pmatrix} - \widetilde{\mathbf{b}}, \qquad \text{if } X \geqslant -x_0,$$

where

$$\widetilde{A} = \begin{pmatrix} a_{11} - \dfrac{b_1}{m} & a_{12} \\ a_{21} - \dfrac{b_2}{m} & a_{22} \end{pmatrix}, \widetilde{\mathbf{b}} = \begin{pmatrix} b_1(1 + \dfrac{c}{m})z_0 \\ b_2(1 + \dfrac{c}{m})z_0 \end{pmatrix}.$$

Starting from these two systems, which form a symmetric pair of dynamical systems, some changes of variables are needed in order to arrive at the system (S_U)-(S_L) of Section 1. Basically, after a rescaling to put the boundary lines at $x = \pm 1$, all what is required is to write the systems in the reduced Liénard form following the approach in [3].

References

[1] M. Akhmet and M.O. Fen, (2016), *Homoclinic and Heteroclinic Motions in Economic Models with Exogenous Shocks*, Applied Mathematics and Nonlinear Sciences, 1, 1–10. doi 10.21042/AMNS.2016.1.00001

[2] A. Andronov, A. Vitt and S. Khaikin, (1966), *Theory of Oscillations,* Pergamon Press, Oxford, doi 10.2307/3613012

[3] E. Freire, E. Ponce and F. Torres, (2014), *A general mechanism to generate three limit cycles in planar Filippov systems with two zones,* Non-linear Dynamics, 78, 251–263, doi 10.1007/S11071-014-1437-7

[4] Yuri A. Kuznetsov, (2004), *Elements of applied bifurcation theory,* Springer-Verlag, New York, 112, doi 10.1007/978-1-4757-3978-7

[5] J. Llibre, (2016), *Centers: their integrability and relations with the divergence,* Applied Mathematics and Nonlinear Sciences, 1, 79–86, doi 10.21042/AMNS.2016.1.00007

[6] R. Lupini, F. Bizzarri and M. Storace, (2001), *Discontinuities in a One-Dimensional Map Describing a Hysteretic Chaotic Circuit,* Non-linear Analysis, 47, 5253–5264, doi 10.1016/S0362-546X(01)00632-0
[7] U. F. Moreno, P. L. D.Peres and I. S. Bonatti, (2003), *Analysis of Piecewise-Linear Oscillators With Hysteresis,* IEEE Trans. Circuits Syst. I, 50, 1120–1124, doi 10.1109/TCSI.2003.815219
[8] K. A. Morris, (2011), *What is Hysteresis?,* ASME Applied Mechanics Reviews, 64, doi 10.1115/1.4007112
[9] T. Saito and K. Mitsubori, (1995), *Control of Chaos from a Piecewise Linear Hysteresis Circuit,* IEEE Trans. Circuits Syst. I, 42, 168–172, 10.1109/81.376872
[10] A. Visintin, (1994), *Differential Models of Hysteresis*, Springer-Verlag, New York.